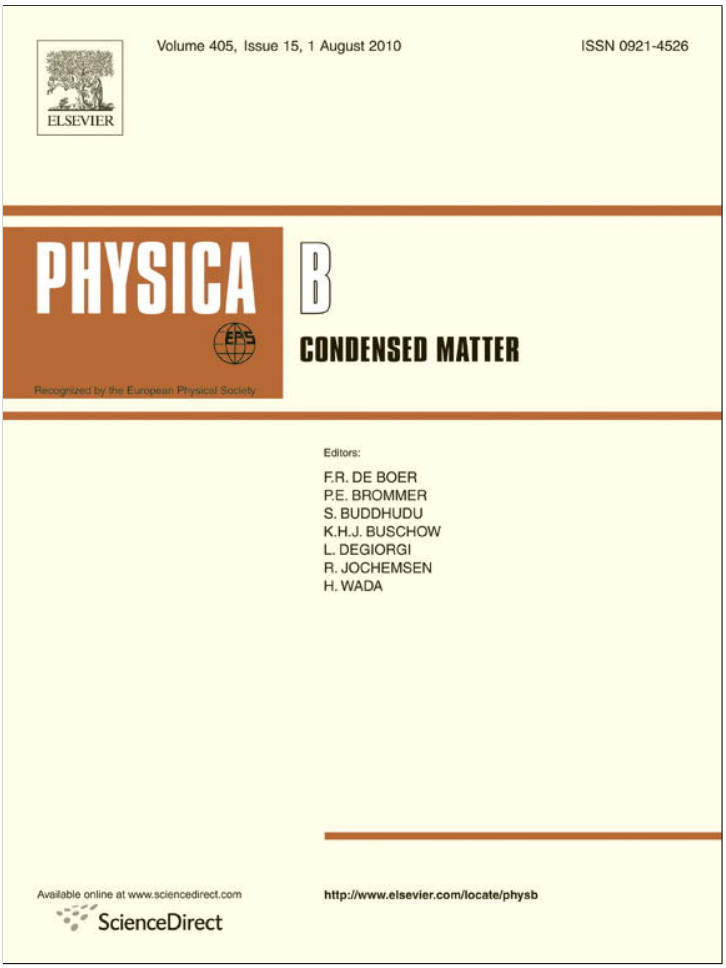

Physica B 405 (2010) 3186–3189

Contents lists available at ScienceDirect

Physica B

journal homepage: www.elsevier.com/locate/physb

Potential fluctuations in $Cu_2ZnSnSe_4$ solar cells studied by temperature dependence of quantum efficiency curves

J. Krustok*, R. Josepson, T. Raadik, M. Danilson

Tallinn University of Technology, Ehitajate tee 5, 19086 Tallinn, Estonia

ARTICLE INFO

Article history:
Received 16 December 2009
Received in revised form
18 February 2010
Accepted 20 April 2010

Keywords:
$Cu_2ZnSnSe_4$
Solar cell
Temperature dependence
Monograin powder
Quantum efficiency curves

ABSTRACT

A new method to study spatial potential fluctuations in compensated absorber materials used in solar cells is introduced. The method is based on the analysis of the temperature dependence of quantum efficiency curves in solar cells. As an example $Cu_2ZnSnSe_4$ monograin solar cell is studied at temperatures $T=10$–300 K. It is shown that this absorber material has spatial potential fluctuations with an average energetic depth of 25 meV. The room temperature bandgap energy of $Cu_2ZnSnSe_4$ is found to be $E_g=1.017$ eV.

1. Introduction

$Cu_2ZnSnSe_4$ (CZTSe) is a p-type semiconductor which could replace $CuInSe_2$ absorber in the future solar cells. In this compound expensive and resource-limited In is substituted by Zn and Sn. Recently a conversation efficiency as high as 9.3% was reported in CZTSe solar cells [1]. Latest studies have shown that the bandgap energy of this compound at room temperature is about 1 eV [2,3]. This is also confirmed by theoretical calculations [4]. An ideal thin-film solar cell absorber material should have a direct bandgap of around 1.3–1.4 eV and therefore one needs to adjust the bandgap energy. One possible way to do so is to use solid solutions with an overall stoichiometry of $Cu_2ZnSn(Se_xS_{1-x})_4$. Unfortunately, the fundamental physical properties of these solid solutions are not well understood. The same is true for CZTSe. Photoluminescence (PL) and Raman studies of this Cu-poor compound [2] showed rather high concentrations of charged point defects. A high defect concentration is typical also for Cu-poor $CuInSe_2$ and other compensated ternary compounds and usually leads to the formation of spatial potential fluctuations [5,6]. As a result, the density of states function for valence and conduction bands has an exponential tail. Potential fluctuations usually form potential wells for holes and thus localized states can be formed. These states can be detected by PL emission, which involves recombination of free electrons with holes localized in these tail states. Usually this emission shows asymmetrical PL bands and from the shape of these PL bands the average depth of potential fluctuations γ can be found [5]. Typically in chalcopyrite ternaries γ has a value below 30 meV [5–7]. Our recent PL studies show that in CZTSe $\gamma \approx 24$ meV [8]. The hole concentration in this absorber was always lower than 10^{16} cm^{-3}, as was detected by C–V measurements. In the present paper we propose a new method to study spatial potential fluctuations in CZTSe. It is based on the analysis of temperature dependent quantum efficiency measurements of solar cells.

2. Experimental

In this study we used monograin solar cells, where the CZTSe absorber in the form of monograins was prepared from CuSe, ZnSe, and SnSe precursors in molten KI. The binary compounds in stoichiometric relation of CZTSe were mixed with KI and ground in a planetary ball mill. The mixture was degassed and sealed into quartz ampoules. The recrystallization temperature was 1000 K. The crystal size was controlled by the temperature and the duration of the recrystallization process. Crystals have a typical diameter of 50 μm. The chemical composition Cu/(Zn+Sn)=0.87; Zn/Sn=0.97 of the monograin powder was determined by the energy dispersive X-ray spectroscopy (EDS). In the record cells composition Cu/(Zn+Sn)=0.8; Zn/Sn=1.22 was reported [1]. In our experiment crystals were Cu-poor and slightly Sn-rich while in record cells [1] Zn-rich composition was used. The CZTSe phase was confirmed by the X-ray diffraction (XRD) measurements. All

* Corresponding author. Tel.: +372 620 3364; fax: +372 620 3367.
E-mail address: krustok@staff.ttu.ee (J. Krustok).

0921-4526/$ - see front matter © 2010 Elsevier B.V. All rights reserved.
doi:10.1016/j.physb.2010.04.041

powder crystals were covered with CdS thin layer by chemical bath deposition. For monograin layer (MGL) formation a monolayer of sieved, nearly unisize grains was bound into a thin layer of epoxy resin, so that the contamination of the upper surfaces of the crystals with epoxy was avoided. After the polymerization of epoxy, a ZnO window layer was deposited onto the front side of the MGL by RF-sputtering. Solar cell structures were completed by vacuum evaporation of a 1–2 μm thick In grid contact onto the ZnO window layer. After glueing the structures on glass substrates, the back contact area of crystals covered with epoxy was opened by etching the epoxy with H_2SO_4 followed by an additional abrasive treatment. The back contact was made using graphite paste. More details about the solar cell preparation can be found in [3].

I–V curves of these solar cells were measured using a Keithley 2400 source meter with the Oriel class A solar simulator 91159A. The typical area of the cells was 3–4 mm^2. For the temperature dependent quantum efficiency measurements solar cells were mounted in a closed cycle He-cryostat (Janis) where the temperature of the cell can be controlled in the range of $T=10$–300 K. A 100 W calibrated halogen lamp was used as a light source together with the a SPM-2 prism monochromator. Monochromatic and modulated (120 Hz) light was focused on the front surface of the solar cell. The generated short circuit current was detected with a DSP Lock-In (SR 810).

3. Results and discussion

A typical *I–V* curve of a CZTSe cell is given in Fig. 1.

It can be seen that this CZTSe cell has quite low solar cell parameters. Especially low is the open circuit voltage V_{oc}. In this cell we assume to have quite big recombination losses. However, we see that even this "bad" cell generates current and therefore it is possible to use it to study the temperature dependence of its quantum efficiency.

The low-energy side of the quantum efficiency spectrum near the bandgap energy E_g of the absorber can be fitted by the equation of Klenk and Schock [9]:

$$QE = K(1-\exp(-\alpha L_{eff})) \quad (1)$$

where $L_{eff}=w+L_d$ is the effective diffusion length of minority carriers, L_d is their diffusion length in the absorber material, w is the width of the depletion region, and α is the absorption coefficient of the absorber material. The constant K is unity in absolute measurements. It is obvious that in the case of a compensated absorber material also the effective diffusion length of majority carriers must be taken into account. Therefore in compensated CZTSe we expect to see a more pronounced role of the hole mobility on the temperature dependence of QE curves.

The fundamental absorption edge in most semiconductors follows an exponential law and for energies $E<E_g$ the absorption coefficient usually can be described by the so-called Urbach rule [10,11]:

$$\alpha(E) = \alpha_0 \exp\left[\frac{\sigma}{kT}(E-E_0)\right] \quad (2)$$

where σ is a steepness parameter, and E_0 and α_0 are characteristic parameters of the material.

Assuming that in this region *QE* is mostly determined by the absorption coefficient, i.e.

$$QE^*E(E) \propto \alpha(E) \quad (3)$$

the *QE*E* curves must also have an exponential part where we are able to find σ, E_0, and α_0. Indeed, Fig. 2 shows the exponential part of the *QE*E* curves at different temperatures.

All these *QE*E* curves were fitted using Eq. (2). From these fits we found E_0 and the temperature dependence of the steepness parameter σ as shown in Fig. 3. It should be mentioned that at low temperatures, where $T<60$ K we have slightly lower E_0 values. One reason for this could be a too low mobility of carriers on the *QE* curve at very low temperatures. Therefore the assumed relation (3) is not valid any more in this temperature region.

The data from Fig. 3 are fitted to the following empirical relation [10,11]:

$$\sigma = \sigma_0(2kT/\hbar\omega_P)\tanh(\hbar\omega_P/2kT) \quad (4)$$

where σ_0 is a constant and $\hbar\omega_P$ the energy of the phonons associated with Urbach's tail. According to fitting results we got $\hbar\omega_P=85$ meV (686 cm^{-1}) and $\sigma_0=1.46$. Our latest Raman measurements showed that the highest phonon energy in CZTSe is about 250 cm^{-1} [2]. It was shown [12–14] that in the case of a structural and electronic disorder the corresponding phonon energy found from Urbach's tail always seems to be much higher than the energy of measured phonon modes. For example, in $CuInSe_2$ phonon energies as high as 60 meV were found from Urbach's tail measurements while the highest optical mode energy obtained from Raman measurements was only 29 meV [14]. Similarly, in our CZTSe crystals with their quite high defect concentrations, the high value of the observed phonon energy

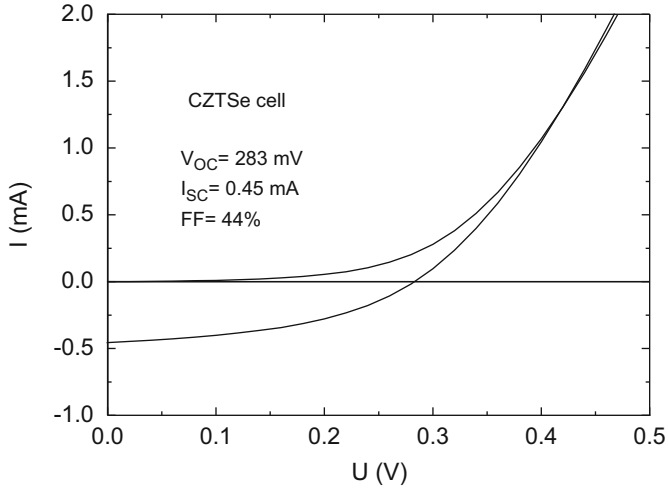

Fig. 1. Dark and light *I–V* curves of CZTSe cell measured at room temperature.

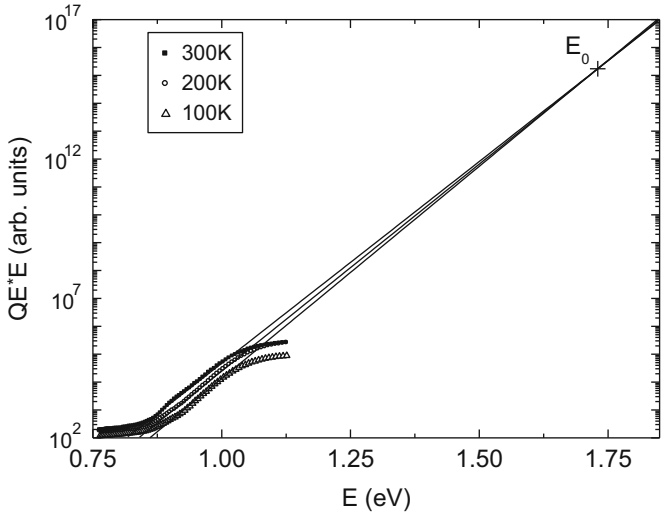

Fig. 2. Typical *QE*E* curves obtained at different temperatures showing the exponential Urbach behaviour with E_0 at 1.73 eV. Solid lines are the fitting results with Eq. (2).

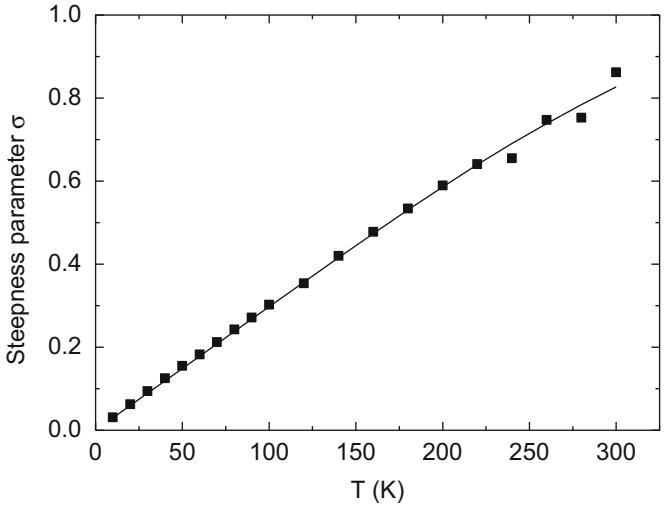

Fig. 3. Temperature dependence of steepness parameter σ. Solid line represents the fit using Eq. (4).

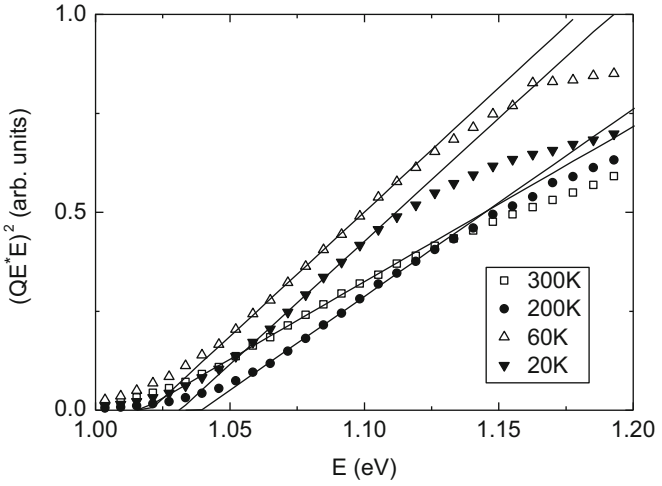

Fig. 4. Normalised QE curves vs. photon energy measured at different temperatures. Solid lines are fits using Eq. (5).

seems to be realistic. The most important result of this kind of analysis is that we really can use *QE* curves to obtain information about the behaviour of the absorption coefficient.

Above the exponential tail, the absorption coefficient of direct band semiconductor has been observed to obey the equation: $\alpha(E) = B(E-E_g)^{1/2}$. If the absorption coefficient is small, i.e. near the bandgap energy $E \approx E_g$, then Eq. (1) can be simplified as

$$QE \approx K\alpha L_{eff} \approx A(E-E_g^*)^{1/2}/E \tag{5}$$

where E_g^* is an effective bandgap energy and constant A includes all parameters that do not depend on E. Therefore $(E^*QE)^2$ vs. E curves should have a linear segment from which one can find a value for E_g^*. In case of spatial potential fluctuations the effective bandgap energy is lower than the bandgap energy of the "ideal" semiconductor without potential fluctuations, because the shape of the $\alpha(E)$ curve does not completely follow the $E^{1/2}$ rule, see for example [15]. Especially at low temperatures, when electrons and holes can occupy localized states inside the potential wells, the difference between E_g and E_g^* can be quite big. At the same time when potential fluctuations are very small we often will find $E_g \approx E_g^*$ [15].

Typical *QE* curves measured at different temperatures are given in Fig. 4. All curves have an $E^{1/2}$ behaviour in the energy range of about $E=1.02$–1.12 eV. From these curves E_g^* was found for every temperature used, see Fig. 5.

It can be seen from Fig. 5 that at low temperatures E_g^* is almost constant but drops at $T=60$ K. At $T>60$ K the effective bandgap energy increases with temperature until at $T \approx 250$ K it starts to decrease again. The overall increase of the E_g^* at $T=60$–250 K is about 23 meV.

This kind of dependence can be explained if we take deep potential fluctuations into account in our sample. It is obvious that *QE* depends not only on the absorption coefficient but also on the ability of generated charge carriers to reach the front and back contacts. Especially at low temperatures the heavier holes tend to localize inside the potential wells. Although at low temperatures we probably have an absorption at $E<E_g$, here the *QE* curves do not show any remarkable current. The reason could be that this spectral region belongs to the deepest potential wells and the generated holes cannot move and hence the *QE* remains small. Therefore we start to measure a current only at higher photon energy, where the potential wells are not so deep and photo-generated holes can move. At higher temperatures also the current generated from the deepest wells increases. They can now

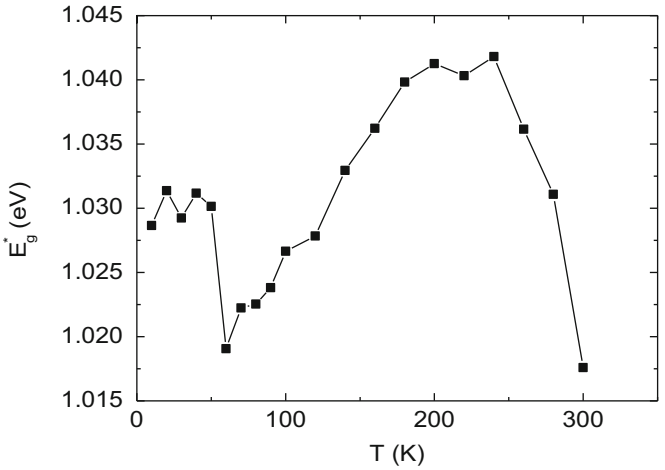

Fig. 5. The temperature dependence of the effective bandgap energy E_g^*.

move and thus we see a small decrease of the effective bandgap energy at $T=60$ K. Because the concentration of these deep wells is small and only a fraction of all charges are liberated we should see here also a decrease in the integrated *QE* at the same temperature. The temperature dependence of the integrated quantum efficiency Φ is given in Fig. 6. In the range of $T=60$–250 K we see an increase of Φ with temperature. It is obvious that this increase is related to thermally activated liberation of charges from the potential wells. If we assume that the average depth of these energy wells is γ, then there must be a temperature region, where

$$\Phi = \Phi_0 \exp(\gamma/kT) \tag{6}$$

Indeed, from the inset of Fig. 6 we see that the fit to Eq. (6) gives $\gamma = 25 \pm 1$ meV. This energetic depth correlates with the shift of E_g^* with temperature in the same region, if we also take the decrease of the bandgap energy with temperature into account. Therefore the observed shift of E_g^* is slightly smaller than γ.

The value of γ found from *QE* curves is actually very close to the corresponding value obtained from photoluminescence measurements, for which $\gamma=24$ meV was determined for our CZTSe crystals [8].

At higher temperatures all charges possess enough activation energy to be free and therefore $E_g^* \approx E_g$. From Fig. 5 we can find the bandgap energy for CZTSe at room temperature to be $E_g=1.017$ eV.

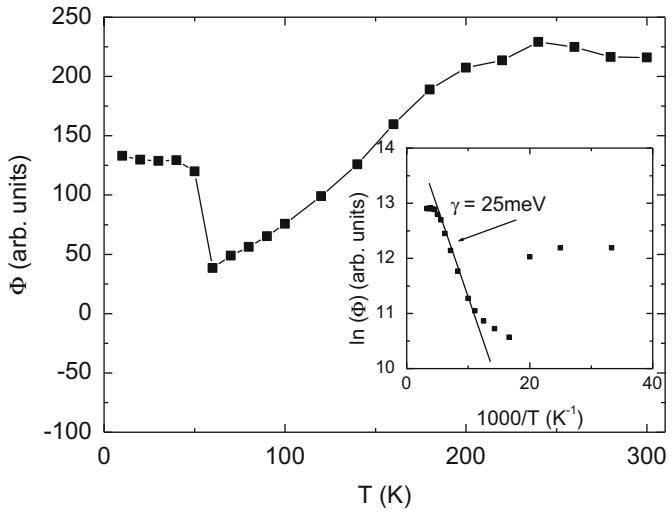

Fig. 6. Temperature dependence of the integrated quantum efficiency Φ. The inset shows an exponential part fitted with Eq. (6).

Our previous PL studies [2] showed that the low temperature bandgap energy of CZTSe must be in the range of 1.02 eV. The bandgap energy obtained from *QE* curves confirms this value. It is obvious that if the concentration of majority carriers (holes) is high. then *QE* is mainly determined by the effective diffusion of minority carriers (electrons). At the same time electrons generally have a smaller effective mass and therefore they usually do not have localized states inside the potential wells. Therefore in this case the temperature dependence of *QE* curves should not show such a pronounced shift of the effective bandgap energy with temperature. Thus this kind of analysis is more suitable for compensated absorber materials and can be used to study spatial potential and probably also compositional fluctuations in these materials.

4. Conclusions

Quantum efficiencies of photocurrent generation in $Cu_2ZnSnSe_4$ monograin solar cell were measured between 10 and 300 K. It was shown that these curves can be used to determine effective bandgap energies of the absorber. The temperature dependence of the effective bandgap energies and of the integrated quantum efficiency dependencies allows to calculate the average depth of potential wells for charge carriers. The such determined value of 25 meV agrees very well with the value determined in photoluminescence measurements. It was shown that the room temperature bandgap energy in $Cu_2ZnSnSe_4$ is $E_g = 1.017$ eV.

Acknowledgements

The authors thank the CZTSSe-team at the TUT. This work was supported by the Estonian Science Foundation grant G-8282 and by the target financing by HTM (Estonia) No. SF0140099s08.

References

[1] T.K. Todorov, K.B. Reuter, D.B. Mitzi, Adv. Mater. 22 (2010) Published Online: 8 February 2010.
[2] M. Grossberg, J. Krustok, K. Timmo, M. Altosaar, Thin Solid Films 517 (2009) 2489.
[3] M. Altosaar, J. Raudoja, K. Timmo, M. Danilson, M. Grossberg, J. Krustok E. Mellikov, Phys. Status Solidi (a) 205 (2008) 167.
[4] ShiYou Chen, X.G. Gong, A. Walsh, S.H. Wei, Appl. Phys. Lett. 94 (2009) 041903.
[5] J. Krustok, H. Collan, M. Yakushev, K. Hjelt, Phys. Scripta T79 (1999) 179.
[6] J. Krustok, J. Raudoja, M. Yakushev, R.D. Pilkington, H. Collan, Phys. Status Solidi (a) 173 (1999) 483.
[7] M. Grossberg, J. Krustok, A. Jagomägi, M. Leon, E. Arushanov, A. Nateprov I. Bodnar, Thin Solid Films 515 (2007) 6204.
[8] M. Grossberg, J. Krustok, J. Raudoja, K..Timmo, M. Altosaar, T. Raadik, Photoluminescence and Raman study of $Cu_2ZnSn(Se_xS_{1-x})_4$ monograins for photovoltaic applications (to be published).
[9] R. Klenk and H.W. Schock, Photocurrent collection in thin film solar cells—calculation and characterization for $CuGaSe_2$/(Zn,Cd)S, in: Proceedings of the 12th Euoropean Photovoltaic Solar Energy Conference, 1994, pp.1588–1591.
[10] F. Urbach, Phys. Rev. 92 (1953) 1324.
[11] G.D. Cody, T. Tiedje, B. Abeles, Y. Goldstein, Phys. Rev. Lett. 47 (1981) 1480.
[12] E. Arushanov, S. Levcenko, N.N. Syrbu, A. Nateprov, V. Tezlevan, J.M. Merino, M. León, Phys. Status Solidi (a) 203 (2006) 2909.
[13] I. Bonalde, E. Medina, M. Rodriguez, S.M. Wasim, G. Marin, C. Rincon A. Rincon, C. Torres, Phys. Rev. B 69 (2004) 195201.
[14] S.M. Wasim, I. Bonalde, E. Medina, G. Marin, C. Rincon, J. Phys. Chem. Solids 66 (2005) 1187.
[15] A.P. Levanyuk, V.V. Osipov, Sov. Phys. Usp. 24 (1981) 187.